

## Application of the disturb and observe algorithm together with a control system for the boost converter in photovoltaic applications

### Aplicación del algoritmo perturbar y observar junto con un sistema de control para el convertidor elevador-boost en aplicaciones fotovoltaica

MÉNDEZ-DÍAZ, Juan Francisco<sup>†\*</sup>, PERALTA-SÁNCHEZ, Edgar<sup>''</sup>, BONILLA-BARRANCO, Hector<sup>'''</sup> and HERNÁNDEZ-SÁNCHEZ, Daniel Eduardo<sup>'''</sup>

<sup>\*</sup> Facultad de Ingeniería Ambiental, Centro de Investigación en Potencia Eléctrica y Energías Limpias. Universidad Popular Autónoma del Estado de Puebla. Puebla, México.

<sup>''</sup> Centro de Investigación en Potencia Eléctrica y Energías Limpias. Universidad Popular Autónoma del Estado de Puebla. Puebla, México.

<sup>'''</sup> Centro de Investigación en Potencia Eléctrica y Energías Limpias. Universidad Popular Autónoma del Estado de Puebla, Centro de Innovación y Desarrollo Tecnológico en computo, Instituto Politécnico Nacional. Puebla, México.

ID 1<sup>st</sup> Author: Juan Francisco, Méndez-Díaz / ORC ID: 0000-0001-6267-3671, CVU CONACYT ID: 292499

ID 1<sup>st</sup> Co-author: Edgar, Peralta-Sánchez / ORC ID: 0000-0001-2602-5025, CVU CONACYT ID: 40745

ID 2<sup>nd</sup> Co-author: Héctor, Bonilla-Barranco / ORC ID: 0000-0002-5020-7312, CVU CONACYT ID: 553622

ID 3<sup>rd</sup> Co-author: Daniel Eduardo, Hernández-Sánchez / ORC ID: 0009-0003-5527-8587, CVU CONACYT ID: 700596

DOI: 10.35429/JEE.2023.18.7.11.26

Received January 15, 2023; Accepted June 30, 2023

#### Abstract

The boost-boost converter presents interesting characteristics for photovoltaic applications, due to the nature of the system where we can increase the voltage in an adequate and controlled way according to the load, in combination with an optimal control system we can obtain a better efficiency of an autonomous photovoltaic system, taking into consideration that a solar panel within its most significant properties to operate within the most efficient way needs natural conditions of irradiation and temperature that are closest to the SCT measurement standard, otherwise efficiency will be lost. Therefore, it is necessary to jointly implement a control system together with an algorithm that allows it to always be in maximum power conditions (MPP). According to the above, this article addresses the low voltage photovoltaic application of an isolated system, using a boost converter and a PI control system, together with an algorithm for obtaining the maximum power point, using two different photovoltaic systems, with the objective of showing that with an essential PI control we can obtain good efficiency of the two systems even with disturbances, as if a more robust control were implemented in photovoltaic applications, saving both operation cost and implementation time. The I-V (current-voltage) characteristics similar to a non-linear source of the photovoltaic module, require the inclusion of linearization of the photovoltaic module and with this to be able to design the control of the system, the proper functioning of the designed control has been tested through mathematical modeling and simulation.

DC/DC converters, Autonomous photovoltaic systems, Control systems, MPPT perturb and observe, Energy efficiency

#### Resumen

El convertidor elevador-boost presenta características interesantes para aplicaciones fotovoltaicas debido a la naturaleza del sistema, por ejemplo, es posible aumentar el voltaje de una manera adecuada y controlada de acuerdo con la carga. En combinación con un sistema de control óptimo podemos obtener una mejor eficiencia de un sistema fotovoltaico autónomo, teniendo en consideración que un panel solar dentro de sus propiedades más significativas para operar dentro de manera más eficiente necesita de condiciones naturales de irradiación y temperatura lo más cercanas al estándar de medida SCT, de no ser así se perderá eficiencia, por lo que es necesario implementar de manera conjunta un sistema de control con un algoritmo que le permita siempre estar en la condiciones de máxima potencia (MPP). De acuerdo con lo anterior, en este artículo se aborda la aplicación fotovoltaica en bajo voltaje de un sistema aislado, utilizando un convertidor elevador-boost, un sistema de control PI y un algoritmo de obtención del punto de máxima potencia. Se utilizan dos sistemas fotovoltaicos diferentes con el objetivo de mostrar que con un control PI esencial podemos obtener buena eficiencia de los ambos sistemas aun con presencia de perturbaciones al igual que si se implementara un control más robusto en aplicaciones fotovoltaicas permitiendo un ahorro tanto de costo de operación como de tiempo en la implementación. Las características I-V (corriente-tensión) similar a una fuente no lineal del módulo fotovoltaico requieren la inclusión de linealización del módulo fotovoltaico y con esto poder diseñar el control del sistema. El funcionamiento del control diseñado ha sido probado mediante el modelado matemático y por simulación.

Convertidores conmutados DC/DC, Sistemas fotovoltaicos autónomos, Sistemas de control, MPPT perturbar y observar, Eficiencia energética

**Citation:** MÉNDEZ-DÍAZ, Juan Francisco, PERALTA-SÁNCHEZ, Edgar, BONILLA-BARRANCO, Héctor and HERNÁNDEZ-SÁNCHEZ, Daniel Eduardo. Application of the disturb and observe algorithm together with a control system for the boost converter in photovoltaic applications. Journal Electrical Engineering, 2023. 7-18:11-26.

\* Correspondence to Author (E-mail: juanfransisco.mendez@upaep.mx)

† Researcher contributing as first author.

## Introduction

In recent years the demand for energy has increased continuously, with the main source being the indiscriminate use of fossil fuels. This constantly growing energy demand has generated an increase in greenhouse gases, causing severe damage to the environment, such as global warming and the worldwide problem of climate change. Thus, in the global energy context, renewable energies have emerged as a response to the social demand to reduce CO<sub>2</sub> emissions and other pollutants of direct action.

Photovoltaic systems are one of the most studied models for obtaining electricity from renewable sources. According to (Ram, et al., 2017), a particularity when using photovoltaic systems for energy production is the fact that the electrical voltage generated by the photovoltaic panels, which has a non-linear relationship with irradiation, so that the maximum voltage generated does not represent the maximum power that the panel can deliver to an electrical load. Given this non-linearity, the maximum power that the PV panel can deliver is a function of the combination of voltage and current in the electrical load.

This non-linearity presented by the solar panels tries to be solved by determining an operating point or maximum power point (MPP) as long as it is at standard measurement conditions (STC). According to the literature, the STC of the solar panel should be at a temperature of 25°C and an irradiation of 1000 W/m<sup>2</sup> on the surface of the panel. The performance of the most promising PV technology should be regulated according to the MPP. The output of the PV system is affected by temperature, irradiation and partial shading. These changes in environmental conditions limit the efficiency and power output of the panel and the measured output of the panel deviates from the desired set point. To improve the MPP there is the Maximum Power Point Tracker (MPPT) as it estimates and controls the MPP. The design of the MPPT system to achieve a regulated output is done using voltage converters and controllers to converge the MPP even under distribution conditions. There are different types of converters and controllers to optimise the efficiency of the PV panel using MPPT (Sharma & Jain, 2015).

As mentioned before, one of the most important parts to obtain higher efficiency of PV systems is the implementation of algorithms to always find the maximum power point in combination with various control strategies (MPPT: MPP tracking). There are several algorithms, among the most used according to the scientific literature are: the Perturb and Observe method, Incremental Conductance, the Constant Voltage method and the Fuzzy Logic method. In this article, each of them will be explained in general terms, except for the Disturb and Observe algorithm, which is the one used in this work and will be explained in more detail.

According to (Ebrahimi & Viki, 2015), DC-DC converters are widely used in renewable energy generation systems such as solar photovoltaic systems, wind systems and in fuel cells, this in order to obtain a correct energy conversion, as shown in figure (1). A solar photovoltaic (PV) power generation system is used in grid-connected applications and in stand-alone or islanded system, where to improve its efficiency, switched converters can also be implemented (Saravanan & Ramesh Babu, 2017). In (Alam & Hoque, 2019) it is proposed that the most suitable power converter to solve the problem of low voltage levels obtained from PV panels is the boost-boost converter; which raises and regulates the output voltage. The input of the boost converter acts as a current source due to the input inductor, which means that it has almost constant input current, which is favourable in PV systems. By interleaving the boost converters, low ripple current is achieved in the input current, output voltage and high power conversion. This topology can be used for the interface connection between the low voltage of the PV array and a high input voltage of the battery bank or any DC load (Taghvaei, *et al.*, 2013).

The boost converter helps to increase the voltage level, improve stability and power factor. In some cases, the converter can also be used as a pre-regulator. It is clear that DC-DC converters require an acceptable and efficient operation for the PV system to be effective and have the least possible energy losses, this also depends directly on the control that is used in the system and ensures the smooth operation of the system even in the presence of disturbances.

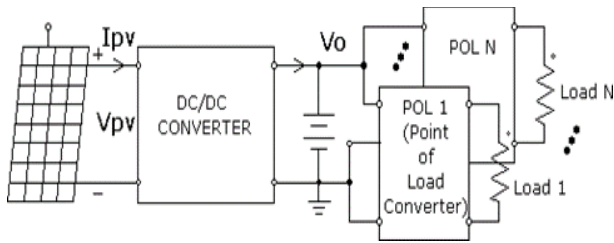


**Figure 1** Photovoltaic system architecture with serial DC bus

Source: Méndez *et al.*, 2014

Another application of boost-boost converter is proposed in (Dhople *et al.*, 2009), where three boost converters are interleaved in which they found superior current characteristics compared to the coupled converters. In (Tian *et al.*, 2016), they use an improved interleaved boost circuit, concluding that this is the most suitable for photovoltaics using an MPPT algorithm, as it has greater advantages than the traditional interleaved boost converter (TIBC) and the single boost converter (SBC) such as:

#### Higher tuning ratio

More stable, accurate output voltage with less ripple.

#### Lower switch voltages

It is useful for increasing system efficiency and reducing energy losses.

According to the above, in order for the operating system to function properly, a control model needs to be developed to enable proper operation. Among the control systems for photovoltaic applications with switched DC/DC converters are Proportional Integral Derivative (PID) and Proportional Integral (PI). According to (Dwivedi & Saket, 2017), in PV system the value of maximum power, current and peak voltage are increased by controlling the gain of PID controller. In (Rabiaa *et al.*, 2019) a cascaded closed-loop control using PI controller is proposed for DC-DC boost converter showing good performance in terms of rise time, disturbance rejection and steady state error.

Furthermore, it is shown that the DC-DC boost converter has a strongly non-linear dynamic behavior, so the performance of any linear controller such as the PI controller can only be optimal as long as the system remains around a certain operating point, i.e. for photovoltaic applications where solar panels are characterized by their non-linear structure, and if a PI or PID control is to be applied, which are controls characterized by using linearized models around an equilibrium point, the behavior of the solar panels must be linearized by means of their basic equation. If this were not the case and it is desired to work with the non-linear structure, other control modes would have to be used, such as the sliding mode control used in (Méndez, *et al.*, 2014; Méndez, *et al.*, 2015; Méndez, 2018 and Méndez, *et al.*, 2019).

Therefore, this article presents the analysis of the boost converter used in two different photovoltaic systems to carry out a comparison between them, implementing a PI control system, with the aim of showing that with an essential control as this widely used in various systems, we can obtain an optimal control performance in the event that disturbances occur, as if it were to implement a more robust control, reducing costs and operating times. Also, to make the system more efficient in combination with PI control, the MPPT Perturb and Observe algorithm is implemented, which helps the PV to operate more efficiently, as it always looks for the point of maximum power. In our application we can obtain the control of the input voltage  $V_{PV}$  of two different PV panels. Considering the parasitic losses that are present in a real system, together with the representative non-linearity of the PV panels. For this reason, the models of both panels are linearized to work around an equilibrium point, to obtain the MPPT even when presenting disturbances, obtaining as a result an optimal response in both systems. The analysis is performed with two different panels with powers of 85 W and 100 W. For the 85 W panel, the article (Méndez *et al.*, 2015) was taken as a reference, where the same panel is used.

The objective of this work can be listed as follows:

To present a general approach to derive the transfer function of the boost-boost DC-DC converter and achieve system control on both solar panels.

Present a PI controller design approach for the input voltage of the PV panels to achieve a constant output voltage independent of the load variation.

Present the implementation of the controller using mathematical modelling and the control system to verify the results of each design.

Demonstrate that with a control such as the PI control, satisfactory results can be obtained in two types of solar panels with different powers, and that these respond appropriately in the event of disturbances in the system.

To implement together with the PI control an MPPT Disturb and Observe algorithm to make the system more efficient.

## Theoretical analysis

### Boost-Boost Converter

The circuit diagram of the boost converter, as shown in figure (2), consists of an electronic switch which is controlled by a pulse width modulation (PWM) signal. The inductor stores the energy coming from the source until the  $T_{on}$  period when the electronic switch is turned on. Meanwhile, when the diode is reverse biased, it isolates the output of the circuit and the load current is supplied from the capacitor (Méndez, *et al.*, 2014). When the electronic switch is off, the inductor is discharged and current flows through the diode. The output voltage is composed of the discharged voltage and the instantaneous panel voltage, so it is always higher than the input voltage. The switch on and off is controlled by the PWM signal (Bouchakour *et al.*, 2015).

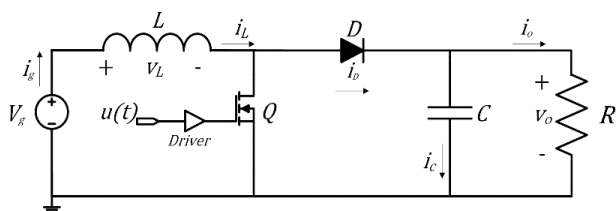


**Figure 2** Schematic of the boost converter  
Source: Méndez, 2018

Therefore, for the research presented in this paper, one of the elementary converters, the boost converter, is used in combination with the solar panel and a battery, which will have a linear behavior as shown in figure (3) and a PI type control is applied together with the MPPT Disturb and Observe algorithm.

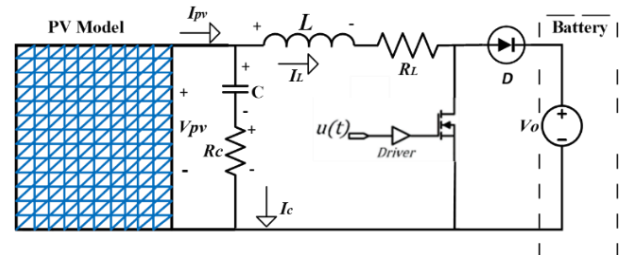


**Figure 3** Performance of a solar panel and battery with a boost converter

Source: Own elaboration

### Analysis of the Photovoltaic Panel, and Maximum Power Point (MPPT)

As expressed in (Leuchter, *et al.*, 2012), photovoltaic panels are non-linear systems, because there is a yield loss that is distributed non-linearly and parametrically (with solar irradiance and temperature) along the panel voltage axis, i.e. the direct application of Shockley's equation,  $I = I_0 * \left[ e^{\frac{v}{n * V_t}} - 1 \right]$ , good modelling results are not available for any panel, and the main reason is the existence of power losses which extend along the voltage axis in a non-linear way.

In addition to these facts, the quality of the semiconductor material  $n$  is also variable and depends on the manufacturing process and the semiconductor material. Other aspects that affect the efficiency of the system are solar radiation and temperature, so when connecting to a DC/DC converter, it is first necessary to linearize the PV panel and then to linearize the converter. The technique for linearizing the converter in this article is performed using state space analysis. For the analysis of the PV systems, we use the parameters from the specification sheets of each PV system, and the classical simplified model of the  $i-v$  relationship of the PV module as shown in figure (4) (Méndez, *et al.*, 2015).

Figure (4) also shows the maximum power point, with the temperature and irradiation factor and the power factor, which as we can see depends directly on external factors such as existing weather changes.

Due to the above, MPPT algorithms must be constantly improved to be more effective and accurate so that external changes to the panel do not significantly affect it (Méndez, *et al.*, 2014; Méndez, *et al.*, 2015; Méndez, 2018 and Méndez, *et al.*, 2019).

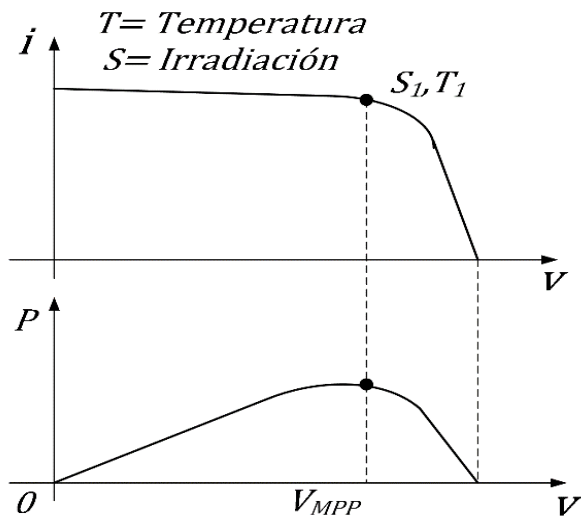


**Figure 4** Maximum Power Point  
Source: Méndez, 2018

As mentioned above, photovoltaic panels must work at maximum power point, for this, several systems and techniques must be related to take advantage of the maximum energy that can be produced, this adaptation must have certain particularities such as: good performance, feasibility, and a dynamic and balanced behavior. As an example of this, figure (5) shows the solar panel in operation, the sensors for measuring both voltage and current, and the integration of the MPPT algorithm together with the direct connection to the converter, and from the converter to the load, which in this case is a battery that has a linear behavior.

With this we begin to guarantee the obtaining of maximum power, where only the control technique is missing, which will help to achieve greater precision and ensure considerable energy production, even if there are sudden changes in temperature, this will be translated as existing disturbances in the system, so the PI controller will have to operate efficiently for optimal work of the PV (Méndez, *et al.*, 2014; Méndez, *et al.*, 2015; Méndez, 2018 and Méndez, *et al.*, 2019).

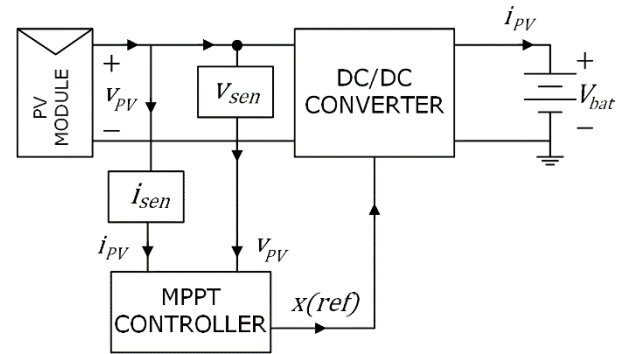


**Figure 5** Switched-mode converter with MPPT  
Source: Méndez, 2018

*Disturb and Observe algorithm and algorithms for obtaining the Maximum Power Point (MPPT)*

- As presented, obtaining the maximum power point MPPT plays a relevant role in the efficiency of solar panels, and therefore, the development of MPPT algorithms becomes paramount.
- One of the most widely used algorithms in the literature is the incremental conductance algorithm. This method is based on the fact that the slope of the power curve versus the voltage generated by the solar panel is zero at the MPP maximum power point, i.e. the maximum power point can be traced by comparing the instantaneous conductance  $I/V$  with the incremental conductance  $\Delta I/\Delta V$ . Among its advantages is its good dynamic response to rapidly changing atmospheric conditions. Its main disadvantage is a higher complexity in the creation of the algorithms compared to other methods. Another algorithm mentioned in the literature is the constant voltage tracking (CVT), this method is based on the intensity of light reflected on the solar panel, when this light intensity is present, the temperature of the panel also changes. At that moment the system measures the voltage produced from the illumination and temperature, and with this it calculates the MPP, and makes it work close to it. This method presents simple, convenient and feasible solutions, but has a disadvantage that it does not operate properly when sudden temperature changes occur.

Another algorithm that is more widely used and is the one employed in this work is the Disturb and Observe algorithm. As shown in figure (6), we have the flow chart of the algorithm which shows the principle of this method based on modifying (perturbing) the operating voltage of the PV array in a certain direction. If the extracted power is increased, it means that the operating point has moved towards the MPP, therefore, the operating voltage should continue to be perturbed in the same direction. If, on the other hand, the power obtained after the perturbation is reduced, it is assumed that the system is moving away from the MPP and the direction of the voltage perturbations must be reversed. The main advantage of this method is that it is easy to implement. Its disadvantage is that the system never operates exactly at the MPP but oscillates around it and the power generated is lower than the theoretical maximum (Méndez, *et al.*, 2014; Méndez, *et al.*, 2015; Méndez, 2018 and Méndez, *et al.*, 2019).

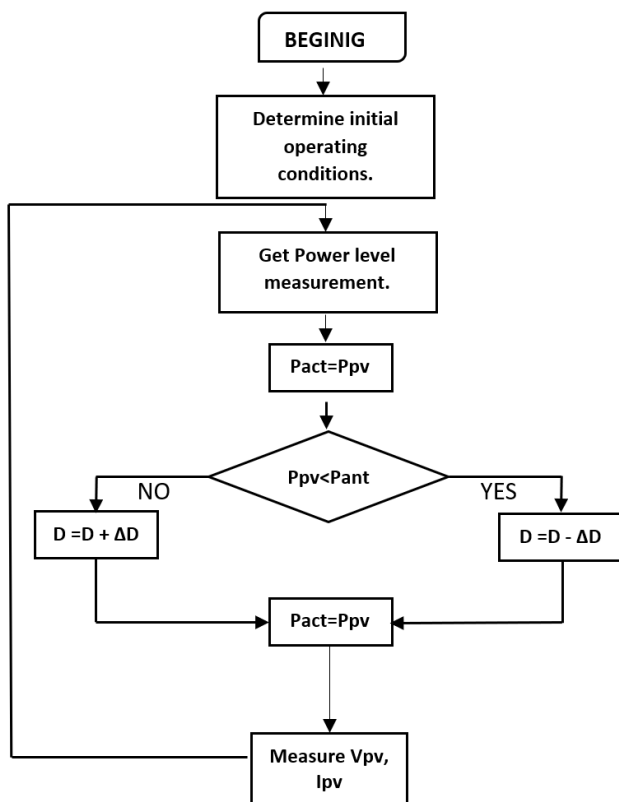


Figure 6 Maximum Power Point Algorithm  
Source: Own elaboration

Solar Panel Linearisation

According to the above, we see the importance of having a good MPPT algorithm interacting with the various systems involved in a PV, but for the mathematical analysis we must linearize the behaviour of our photovoltaic panel as shown below, starting with the analysis of the classical equation of the solar panel, to then implement the control system along with the perturb & observe algorithm.

The classical solar panel equation as shown in equation 1 is as follows:  $i_{pv}$  is the current supplied by the PV module,  $i_s$  is the short circuit current which depends on the irradiance,  $v_{pv}$  is the operating voltage of the module,  $I_R * e^a$  are parameters of the PV module which depend on multiple technological factors and temperature, as shown in figure (7a).

$$i_{pv} = i_{sc} - I_R * e^{a*v_{pv}} \tag{1}$$

To linearize the system we represent it as shown in figure (7b), where the resistor will have the same current and voltage as the classical PV model as found in equation 2, always working at the maximum power point of the MPPT panels.

$$R_{pv} = \frac{v_{mpp}}{i_{pv} - i_{mpp}} \tag{2}$$

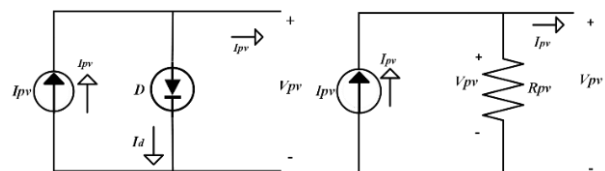
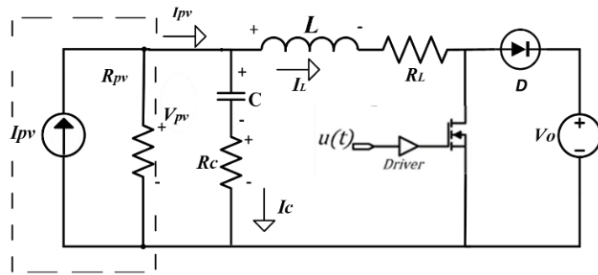


Figure 7a. Figure 7b. Sample of a photovoltaic module with current and voltage variation.  
Source: Own elaboration

Based on what has been seen, for the analysis of the system the Norton model is used, already linearised together with the boost converter as shown in figure (8), and thus be able to perform the mathematical modelling around the MPPT maximum power point as proposed by (Hogan, 2014). Circuits comprising arbitrarily complicated sets of voltage sources, current sources, resistors, capacitances and inductances can be represented by Norton equivalent circuits-

According to the above, we see the importance of having a good MPPT algorithm interacting with the various systems involved in a PV, but for the mathematical analysis we must linearise the behaviour of our photovoltaic panel as shown below, starting with the analysis of the classical equation of the solar panel, to then be able to implement the control system together with the perturb & observe algorithm.



**Figure 8** Norton model in a boost converter

Source: Own elaboration

### Mathematical analysis

For the mathematical analysis of the system, the objective is to control the input voltage of the PV panel and produce the maximum power, based on the boost converter and considering the losses in both the inductor and the capacitor, adding the series resistors in each of the devices.

For the system analysis, it was performed at two operating points, according to the configuration of the boost converter as shown in figure (8).

To obtain the averaged system, we analysed the boost-boost converter, first in switched mode in its two operations, obtaining the following equations:

$$\begin{cases} u = 1 \text{ in state on} \\ u = 0 \text{ in state off} \end{cases}$$

"**u = 1**" Interval 1 (switch closed ON)

$$L \frac{dI_L}{dt} = V_C + I_C \times R_C - I_L \times R_L \quad (3)$$

$$C \frac{dV_C}{dt} = I_C = I_{PV} - I_L \quad (4)$$

"**u = 0**" Interval 2 (switch open OFF)

$$L \frac{dI_L}{dt} = V_C + I_C \times R_C - V_O - I_L \times R_L \quad (5)$$

$$C \frac{dV_C}{dt} = I_C = I_{PV} - I_L \quad (6)$$

Taking into consideration that the generated current  $I_{PV}$  and voltage  $V_{PV}$  of the Norton model represented in figure (8) are not equations of state as shown in equations (4) and (6) in the analysis of the interval when  $u=1$  and  $u=0$ , these will have to be equated so that the current and voltage of the model are equations of state, by equating these two variables with respect to the Norton model in figure (8) we are left with equations (7) and (8):

$$I_{PV} = I_{SC} - \frac{V_{PV}}{R_{PV}} \quad (7)$$

$$V_{PV} = V_C + I_C \times R_C \quad (8)$$

Substituting equations (7) and (8) into (4) we obtain the following equation which is the same for both system states:

$$C \frac{dV_C}{dt} = \frac{1}{R_{PV} + R_C} (I_{SC} \times R_{PV} - I_L \times R_{PV} - V_C) \quad (9)$$

By performing the relevant operations on equations (3) and (5) for the inductor and (9) for the capacitor in the boost converter, the averaged model looks as follows, where the equations are already a function of the system inputs:

$$L \frac{dI_L}{dt} = V_C + I_C \times R_C - I_L \times R_L - V_O \times (1 - d) \quad (10)$$

$$C \frac{dV_C}{dt} = \frac{1}{R_{PV} + R_C} (I_{SC} \times R_{PV} - I_L \times R_{PV} - V_C) \quad (11)$$

For the steady state analysis, we again consider the Norton model of figure (8) where we study the following points according to the electrical structure of the PV system: taking into account that the average capacitor current is zero, we obtain that the inductor current will be equal to the PV panel current and the maximum power current, the same would be for the panel voltage which will be equal to the capacitor voltage and the maximum power voltage, thus obtaining the following equations (12 and 13).

$$I_L = I_{PV} = I_{MPP} \quad (12)$$

$$V_C = V_{PV} = V_{MPP} \quad (13)$$

From the above we can also derive the duty cycle by equating equation (10) to zero resulting in equation (14).

$$D = 1 - \frac{V_{MPP} - I_{MPP} \times R_L}{V_O} \quad (14)$$

Based on the averaged model, the equations of state and the steady state analysis, we can perform the mathematical modelling using the state space analysis, this analysis is performed for both solar panels, where we define the state vectors  $x$ , which are the inductor current  $I_L$  and the capacitor voltage  $V_C$ , the input vectors  $u$ , which are the duty cycle  $d$  the output voltage  $V_O$  together with the panel current  $I_{PV}$  and the control variable  $y$ , which is the PV panel voltage  $V_{PV}$  as shown in the following equation.

$$x = \begin{bmatrix} I_L \\ V_C \end{bmatrix} u = \begin{bmatrix} d \\ V_O \\ I_{PV} \end{bmatrix} y = [V_{PV}] \quad (15)$$

According to equations (10) and (11) and to the vectors presented in (15), the matrix  $\delta$  gives us the relationship between the functions and the states, obtaining as a result the following:

$$\delta = \begin{bmatrix} \left(\frac{1}{L}\right) * \left(\frac{-R_{PV} * R_C}{R_{PV} + R_C}\right) - R_L & \left(\frac{1}{L}\right) * \left(1 - \frac{R_C}{R_{PV} + R_C}\right) \\ \left(\frac{1}{C}\right) * \left(\frac{-R_{PV}}{R_{PV} + R_C}\right) & \left(\frac{1}{C}\right) * \left(\frac{-1}{R_{PV} + R_C}\right) \end{bmatrix} \quad (16)$$

Taking equations (10) and (11) with respect to the input vectors  $u = \begin{bmatrix} d \\ V_O \\ I_{PV} \end{bmatrix}$  for the matrix  $\beta$  which gives us the relationship between the function and the inputs, we obtain:

$$\beta = \begin{bmatrix} \left(\frac{1}{L}\right) * V_O & \left(\frac{1}{L}\right) * (-1 - d) & \left(\frac{1}{L}\right) * R_C \left(\frac{R_{PV}}{R_{PV} + R_C}\right) \\ 0 & 0 & \left(\frac{1}{C}\right) * \left(\frac{R_{PV}}{R_{PV} + R_C}\right) \end{bmatrix} \quad (17)$$

For the matrix  $\gamma$ , having the variable to control  $y = [V_{PV}]$  in terms of the states  $x = \begin{bmatrix} I_L \\ V_C \end{bmatrix}$  we obtain:

$$\gamma = \left[ R_C \left( \frac{-R_{PV}}{R_{PV} + R_C} \right) \quad 1 - \frac{R_C}{R_{PV} + R_C} \right] \quad (18)$$

For the matrix  $D$ , having the variable to be controlled  $y = [V_{PV}]$  on the basis of the entries  $u = \begin{bmatrix} d \\ V_O \\ I_{PV} \end{bmatrix}$  we obtain:

$$\varepsilon = \left[ 0 \quad 0 \quad R_C \left( \frac{R_{PV}}{R_{PV} + R_C} \right) \right] \quad (19)$$

As we can see, the state space analysis shows us the complete behaviour of the system to then obtain the transfer functions for both photovoltaic panels, these functions will be explained in the following section.

Comparison between Proportional, Proportional Integral and Proportional Integral Derivative Controls

As we know, to control a variable of a switched converter, it is necessary that the switched converters have a closed loop control system as shown in figure (9), where 4 components can be observed, 1) the main component, which is the switched converter, and 2) the block that calculates the error of the switching converter, 2) the block that calculates the voltage error  $e(t)$  which is indispensable for the comparison of the system between what is to be controlled and the error  $e(t)$  itself, 3) the control component which mainly acts on the error by amplifying it and 4) the modulator, which transforms the output of the controller into digital signals where they are applied directly to the switches of the switched converter. The modulator block is sometimes considered to be part of the controller block or the plant itself (Méndez, 2018).

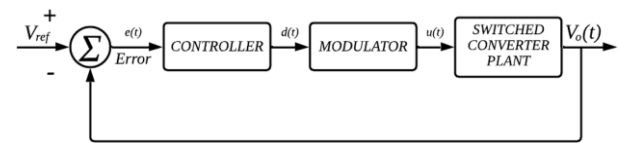


**Figure 9** Control block diagram of a switched regulator  
Source: Méndez, 2018

Based on the above, for the control design presented in this research we have to consider the following: control the input voltage of the solar panel according to the Norton model, always looking for the maximum MPPT power point together with the control system as shown in figure (10), this will be explained in detail in the following section.



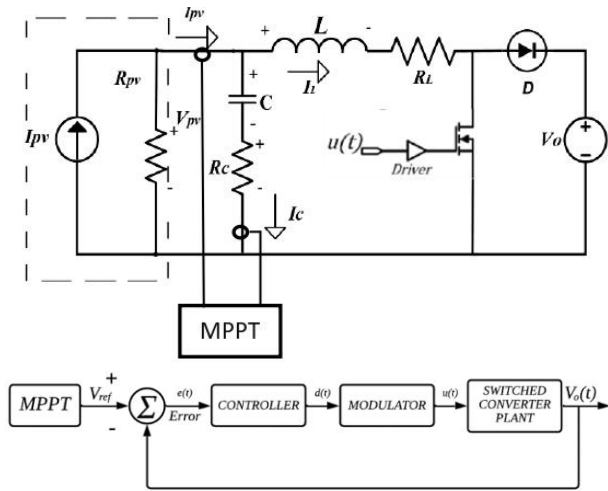


**Figure 10** Control block diagram of a switched regulator together with MPPT input  
 Source: Méndez, 2018

We start with the comparison between the different control systems, explaining why the PI integral proportional control is the one that best suits the needs of the PV system, according to the mathematical analysis explained in the previous section.

*Proportional control panel 85W*

When proportional control is applied, we can see the following:

Working in closed loop, in figure (11) we can see that it is divided into three parts, the step response, the geometric place of the roots and the Bode diagram: In the Bode diagram we can see that when applying the proportional control the bandwidth never reaches the final value, which is marked by the black line and is the value indicated by the control, in the geometric locus of the roots we can see that the closed-loop poles also do not approach the damping (delimited by the black lines) indicated by the control system even when changing the value of the proportional constant, and although we can see that the response over time reaches a certain stability, at start-up it tends to be oscillatory, so we conclude that proportional control is not a good option for implementation in our system.

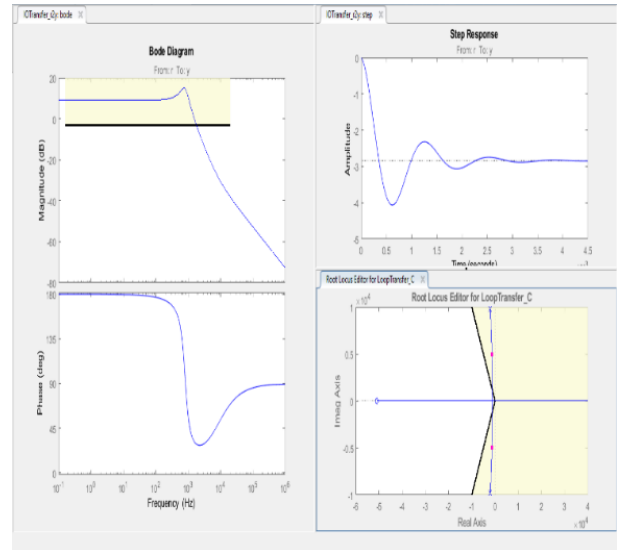


**Figure 11** Application of Proportional Control  
 Source: Own elaboration

*Integral proportional derivative control panel 85W*

When proportional integral derivative control is applied, we can see the following: in figure (12), we can see in the Bode diagram that the bandwidth does reach the value marked by the control line, but although it complies in this way, graphically we can see that the response is not optimal, in the geometric location of the roots we see that the closed-loop poles are not close to the damping marked by the black lines and that it is difficult to reach it. The response over time, like the proportional control, shows a certain stability, but the response at the start of the system also shows some oscillation.

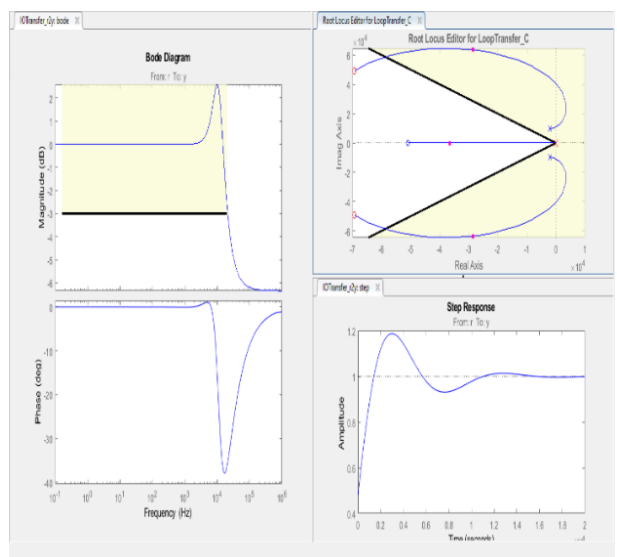


**Figure 12** Application of Derivative Proportional Integral Control  
 Source: Own elaboration

*Integral proportional control panel 85W*

When the proportional integral control is applied, we can see the following:

According to figure (13), as with the two previous controls, it is shown in the Bode diagram that the bandwidth does reach the value marked by the control line, as does the PID control, but it can be seen that the response is optimal, in the geometric location of the roots we see that the closed-loop poles are now positioned directly on the damping lines marked by the control. The response in time presents a stability and an optimum response for the control system, so we can conclude that the PI control compared to the other controls is the optimum in all the operating conditions that the control system designed.

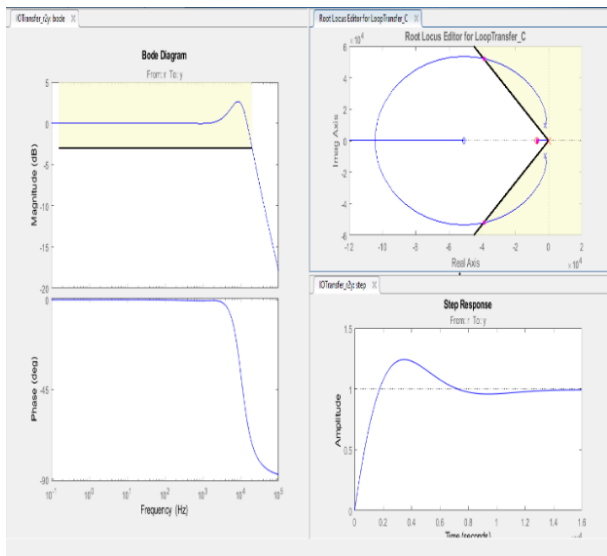


**Figure 13** Application of Derivative Proportional Integral Control  
Source: Own elaboration

*Integral proportional control panel 100W*

When proportional control is applied, the following can be seen:

In figure (14) as in the 85W panel working in closed loop: In the Bode diagram we can see that when applying the proportional control the bandwidth never reaches the final value which is marked by the black line and is the value indicated by the control, in the geometrical place of the roots we can observe that the closed loop poles also do not approach the damping (marked by the black lines) indicated by the control system, even changing the value of the proportional constant we do not have a significant approach, and although we see that the response over time reaches a certain stability, at start-up it tends to be oscillatory, so we conclude that the proportional control is not a good option for implementation in our system, very similar to the behavior in the 85W panel.

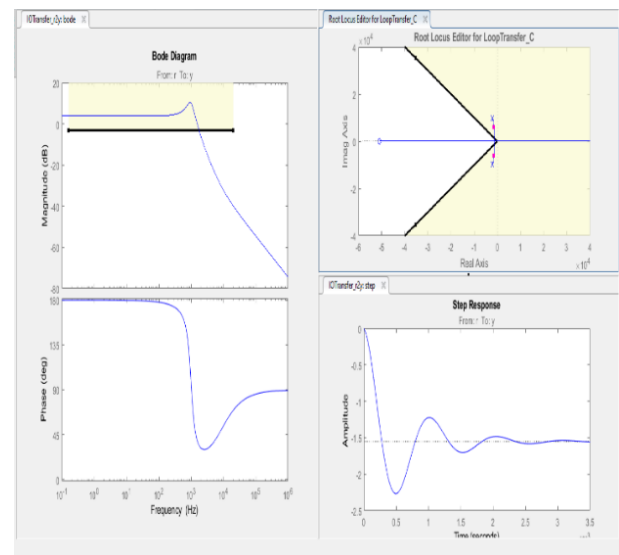


**Figure 14** Application of Proportional Control 100 W  
Source: Own elaboration

*Integral proportional derivative control 100W panel*

When proportional integral derivative control is applied, we can see the following:

In the same way we analyze the system presented in figure (15), very similar to the behavior of the 85W panel, so we will summarize it a little, the Bode diagram the bandwidth does reach the value marked by the control line, but although it complies in this way, graphically it can be seen that the response is not the optimum, in the geometrical place of the roots, the closed loop poles are not close to the damping marked by the black lines, and the response in time as well as the proportional control finds some stability but the response at the beginning of the system also presents some oscillation.

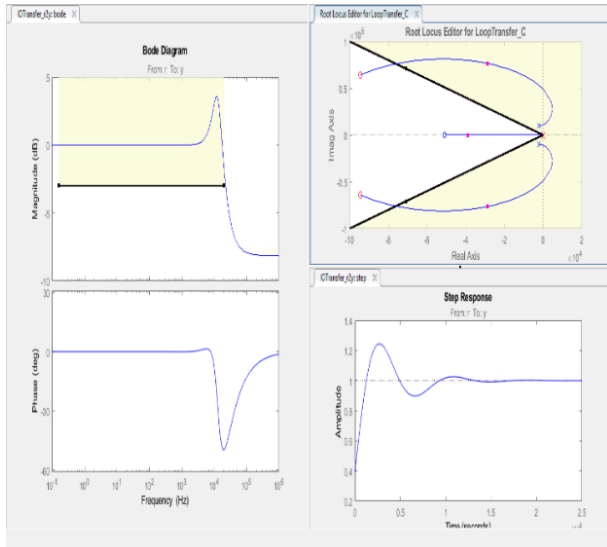


**Figure 15** Application of proportional integral derivative proportional control 100 W  
Source: Own elaboration

*Integral proportional control panel 100W*

When the proportional integral control is applied, we can see the following:

According to figure (16), following the same thematic and observing that the behaviour of the control is also very similar to the 85W panel, we can appreciate that in the Bode diagram the bandwidth does reach the value marked by the control line, just like the PID control but it can be observed that the response is optimal, In the geometric location of the roots we see that the closed-loop poles are now positioned directly on the damping lines marked by the control, and the response over time shows stability and an optimum response for the control system, so we can conclude that the proportional integral control is the most optimum for both panels as it meets the operating conditions required by the control system.

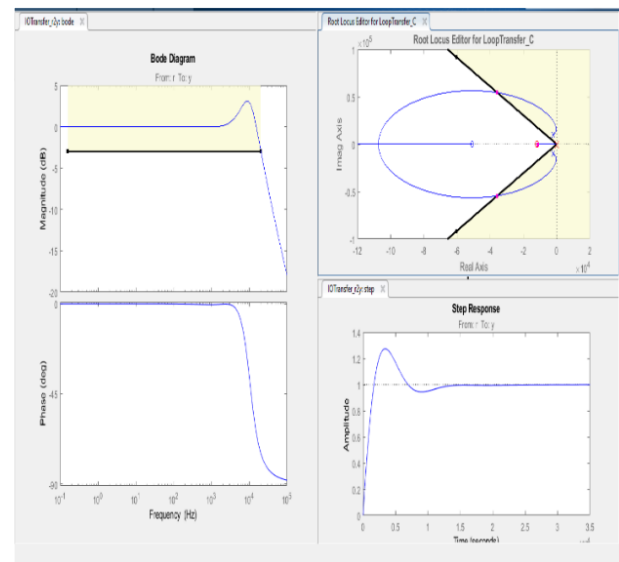


**Figure 16** Application of integral proportional control 100 W  
Source: Own elaboration

*Implementation of control systems*

Based on (Méndez, et al., 2015) for the analysis of the first panel we obtain the following technical characteristics; the photovoltaic panel is an 85 W module, with nominal parameters at 25°C and 1 kW / m2 of:  $ISC = 5$  A,  $Voc = 22.1$  V,  $IMPP = 4.72$  A,  $VMPP = 18$  V. The second panel has the following technical characteristics; it is a 100 W photovoltaic panel with nominal parameters at 25°C and 1 kW / m2 of:  $ISC = 5.86$  A,  $VOC = 22.3V$ ,  $IMPP = 5.38$  A,  $VMPP = 18.6$  V. After the relevant analyses to obtain the parameters of the boost converter, the values for each of the components are as follows:  $L=75\mu H$ ,  $RL=150m\Omega$ ,  $C=75\mu F$ ,  $RC=196.3m\Omega$ .

Obtaining the transfer functions by performing the analysis prior to modelling the boost converter and linearizing around the operating point in both photovoltaic panels is as follows:

For the 85W panel

$$Gvd = \frac{-62641(s+6.791 \cdot 10^4)}{s^2+4817s+1.776 \cdot 10^8} \tag{20}$$

For the 100W panel

$$Gvd = \frac{-62515(s+6.791 \cdot 10^4)}{s^2+4947s+1.776 \cdot 10^8} \tag{21}$$

As we can appreciate both transfer functions are very similar, both show that the system is stable, but they present a negative gain, so the system could present some instability, due to this, the control design becomes more complex, as it is left with positive feedback. The control design now must compensate or cancel the negative gain of the system, and with this, have a stable system. By compensating the gain and as shown in the diagrams above from the comparison of the different controls we get the following transfer functions

For the 85W panel

$$G_{cv} = \frac{-1.6317s - 6773}{s} \quad (22)$$

For the 100W panel

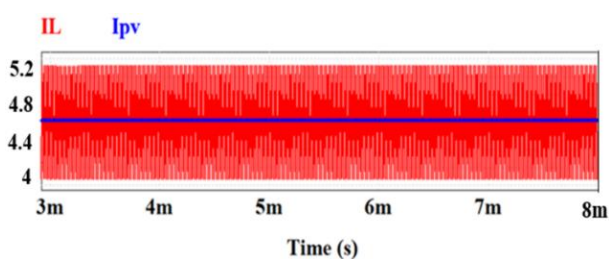
$$G_{cv} = \frac{-1.7511s - 1.42 \cdot 10^4}{s} \quad (23)$$

By obtaining the above transfer functions and with the control system applied, we observe that it is completely stable, which allows the objective of the control system to be achieved, which is to regulate the input voltage of the photovoltaic panel following a reference voltage, always looking for the point of maximum power. As shown in the following graphs, we start with the 85W panel and then the 100W panel.

As we can see in figures (17) and (18), the panel operates properly, which proves that the linearisation of the panel is correct, as it is above 18V, which is the optimum operating voltage of the panel according to its technical data sheet, as well as the panel current  $I_{pv}$  with a value of 4.72A. We can also observe that it is equal to the inductor current, also fulfilling the IL steady state analysis.

For 85W panel

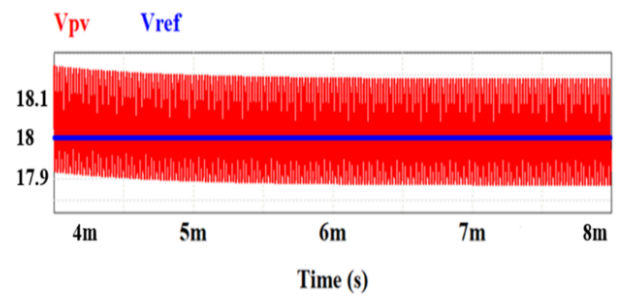
Steady state analysis:



**Figure 17** Steady state analysis

Source: Own elaboration

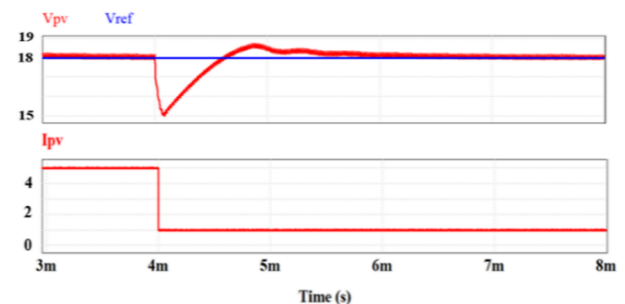
Implemented Control System



**Figure 18** Panel Voltage  $V_{pv}$  and Reference Voltage  $V_{ref}$   
Source: Own elaboration

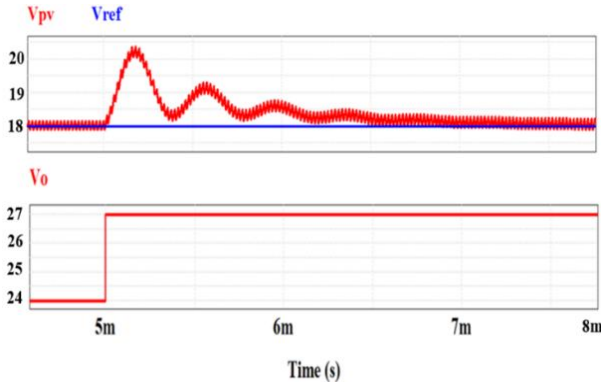
In figure (18) we can see that the control operates properly as the panel voltage  $V_{pv}$  smoothly follows the reference voltage  $V_{ref}$  equal to 18V, always guaranteeing the maximum power point.

Figure (19) shows a direct disturbance to the system simulating a partial shading of the solar panel of almost 70%. The control, when presented with this disturbance, adapts almost immediately and responds again in an optimal way, where it is seen that the voltage  $V_{pv}$  of the solar panel after the disturbance continues without problems to the reference voltage  $V_{ref}$  always above 18 V, taking into account that the disturbance is quite high the control continues to respond adequately.



**Figure 19** Disturbance present simulating partial shading  
Source: Own elaboration

Figure (20) shows another disturbance where there is an increase in the battery voltage due to the load coming from the photovoltaic panel and as can be seen there is an increase in the output voltage  $V_o$  from 24V to 27V and again the solar panel voltage  $V_{pv}$  follows without any complication the reference voltage  $V_{ref}$  always over 18V adapting quickly after the disturbance.



**Figure 20** Second disturbance present in the battery  
Source: Own elaboration

In the same way as in the 85W solar panel, we can see in figures (21) and (22) now with the 100W solar panel, that it operates properly, which also proves that the linearisation of the panel is correct, as it is above 18.6V and the panel current  $I_{pv}$  is equal to the inductor current  $I_L$ , also proving the optimal analysis in steady state.

**100W panel**

**Steady state analysis**

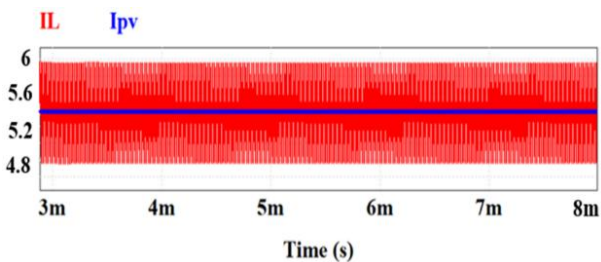


**Figure 21** Steady state analysis  
Source: Own elaboration

*Implemented Control System.*

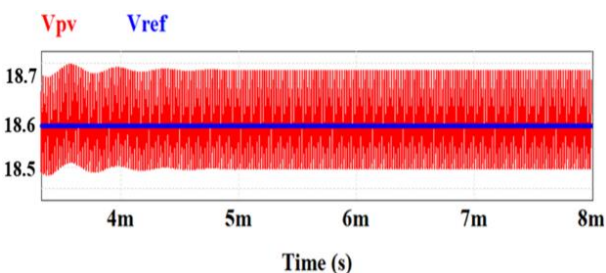


**Figure 22** Panel Voltage  $V_{pv}$  and Reference Voltage  $V_{ref}$   
Source: Own elaboration

As in the previous panel in figure (22) we can see that the control operates properly as the panel voltage  $V_{pv}$  smoothly follows the reference voltage  $V_{ref}$  now at 18.6V, always ensuring the maximum power point, and the stability of the system.

In figure (23) we repeat the same perturbation that was used in the 85W panel, causing a partial shading of the same magnitude, but now in the 100W panel. As we can observe the  $I_{pv}$  current drops its amperage suddenly and considerably, and the control continues to operate correctly, showing the good performance also for this panel.

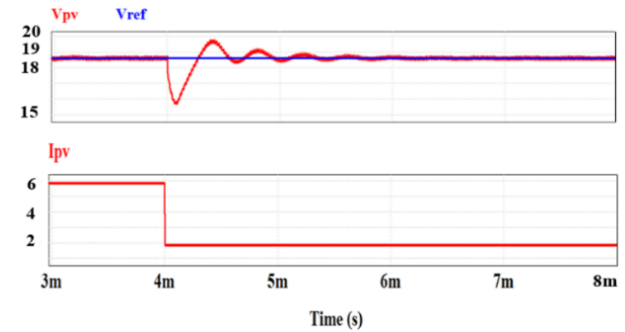


**Figure 23** Disturbance present simulating partial shading  
Source: Own elaboration

Following the same tests as for the 85W panel, we now show the second disturbance in figure (24) for the 100W panel. The battery load is increased and we observe that the control continues to operate correctly, as the panel voltage  $V_{pv}$  continues smoothly at the reference voltage  $V_{ref}$  now at 18.6V.

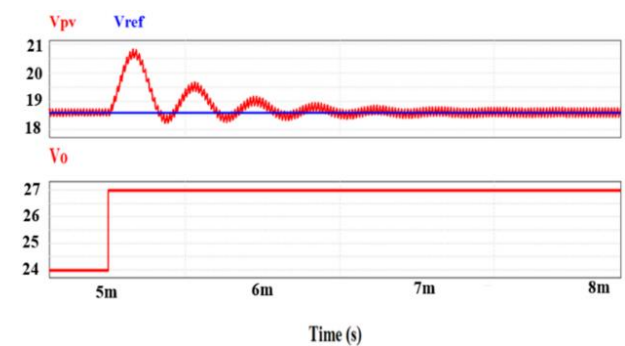


**Figure 24** Second disturbance present in the battery

**Implementation of the maximum power search algorithm perturb and observe**

As we have explained, the techniques for the application of maximum power algorithms are widely used in photovoltaic systems, with the aim of improving the performance of the power output of the photovoltaic system, by constantly monitoring the maximum power point that is directly related to the incidence of radiation and temperature variability in the solar panel. One of the most widely used techniques in photovoltaic systems to obtain maximum power is the perturb and observe algorithm, because it has several advantages, such as low cost and ease of implementation.

In accordance with what has been seen, this article shows the MPPT algorithm based on (Méndez et al., 2015), which is the perturb and observe algorithm, together with the control system already simulated and with the real operation of a solar panel. In the following, the explanation of the perturb-and-observe algorithm is complemented.

The algorithm compares the power obtained for two voltage setpoints separated by a small voltage differential of  $\pm 500$  mV. Every 200  $\mu$ s the voltage setpoint and power of the first point are replaced by those of the second point, while the voltage setpoint of the second point is obtained by adding the differential to its previous value. The algorithm changes the sign of the differential each time the power of the second point is no longer higher than that of the first point.

Following the same format as the previous figures, we will start by showing the behavior of the 85W panel and then the 100W panel including the implementation of the algorithm.

*For the 85W panel*

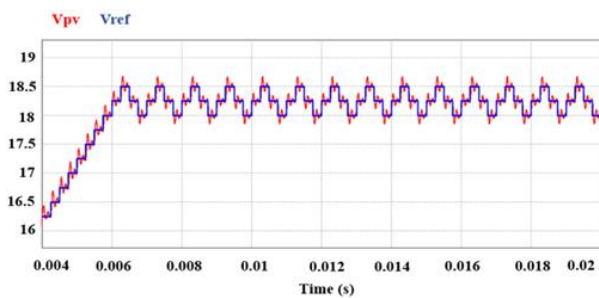


**Figure 25** Implementation of the algorithm with the control system Panel Voltage Vpv and Reference Voltage Vref

As we can see in figure (25) by adding the MPPT algorithm to the control system, it works correctly, as the voltage Vpv smoothly follows the reference voltage Vref always looking for the maximum power point of the solar panel.

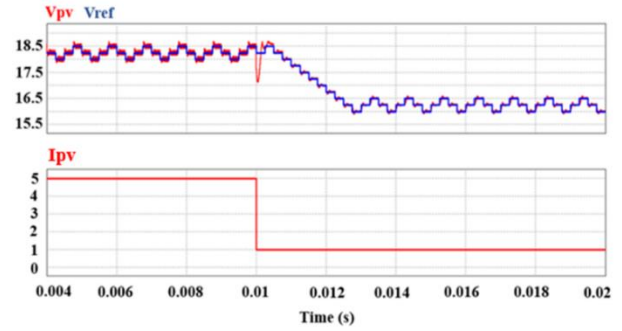


**Figure 26** First disturbance present on the solar panel simulating partial shading

Figure (26) shows again a direct disturbance to the system simulating a shading on the solar panel. The control, when presenting this disturbance, adapts almost immediately and responds again in an optimal way, where it can be seen that the voltage Vpv of the solar panel after the disturbance follows without problems the reference voltage Vref, and always looking for the point of maximum power of the MPPT system.

*For 100w panel*

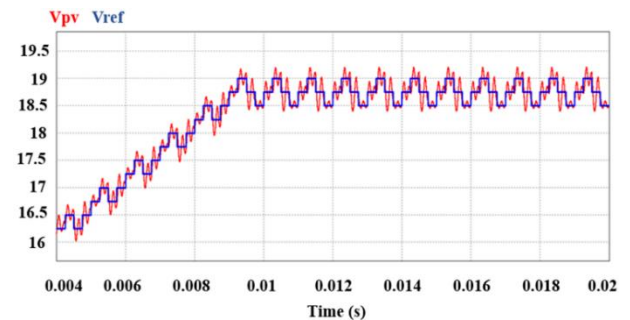


**Figure 27** Implementation of the algorithm with the control system Panel voltage Vpv and Reference voltage Vref

As with the 85W solar panel, we can now see on the 100W solar panel that the control together with the application of the MPPT algorithm works correctly.

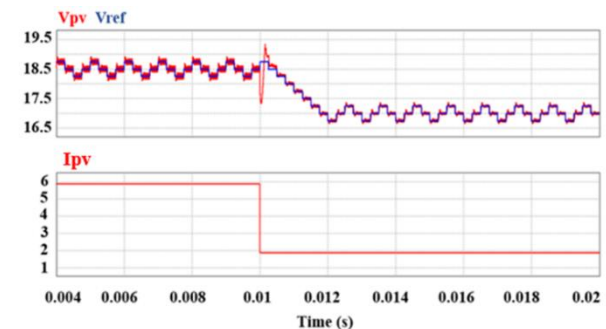


**Figure 28** First disturbance present in the solar panel simulating partial shading

The same test that was performed for the 85W solar panel is performed for the 100W panel, provoking a severe disturbance simulating a partial shading and we can observe in figure (28) that the control operates optimally together with the MPPT algorithm, always looking for the maximum power point.

## Conclusion

Following the theoretical analysis and verifying with the simulations, we can observe that it is possible to regulate the input voltage of the two photovoltaic panels with the application of a PI controller together with the implementation of the perturb and observe algorithm. Using the MATLAB tool for the design itself, we can deduce that the use of this tool greatly facilitates the design of controllers for application in switched-mode converters, and that it fulfils the objectives set out for this research in an optimal manner. It was also found that by implementing a conventional PI control we can have the same performance of a much more robust control, applied to photovoltaic systems, and that in conjunction with the algorithm proposed in this work, for example, good results are obtained regardless of the existence of disturbances, always operating at the point of maximum power, and as a complement, having other advantages such as easy application, reduced operating time and reduced operating costs when required to implement the model physically.

## References

- Ram, J. P., Babu, T. S., & Rajasekar, N. (2017). A comprehensive review on solar PV maximum power point tracking techniques. *Renewable and Sustainable Energy Reviews*, 67, 826–847. <https://doi.org/10.1016/j.rser.2016.09.076>
- Sharma, C., & Jain, A. (2015). Modeling of buck converter models in MPPT using PID and FLC. *Telkomnika (Telecommunication Computing Electronics and Control)*, 13(4), 1270–1280. <https://doi.org/10.12928/TELKOMNIKA.v13i4.1774>
- Ebrahimi, M. J., & Viki, A. H. (2015). Interleaved high step-up DCDC converter with diode-capacitor multiplier cell and ripple-free input current. *International Journal of Renewable Energy Research*, 5(3), 782–788. <https://doi.org/10.11591/eei.v4i4.512>
- Saravanan, S., & Ramesh Babu, N. (2017). Analysis and implementation of high step-up DC-DC converter for PV based grid application. *Applied Energy*, 190, 64–72. <https://doi.org/10.1016/j.apenergy.2016.12.094>
- Alam, K., & Hoque, A. (2019). Design and Analysis of Closed Loop Interleaved Boost Converter with Arduino based Soft PI Controller for Photovoltaic Application. *Proceedings of 2019 3rd IEEE International Conference on Electrical, Computer and Communication Technologies, ICECCT 2019*, 1–5. <https://doi.org/10.1109/ICECCT.2019.8869408>
- Taghvaei, M. H., Radzi, M. A. M., Moosavain, S. M., Hizam, H., & Hamiruce Marhaban, M. (2013). A current and future study on non-isolated DC-DC converters for photovoltaic applications. *Renewable and Sustainable Energy Reviews*, 17, 216–227. <https://doi.org/10.1016/j.rser.2012.09.023>
- Dhople, S. V., Davoudi, A., & Chapman, P. L. (2009). Steady-state characterization of multi-phase, interleaved Dc-Dc converters for photovoltaic applications. *2009 IEEE Energy Conversion Congress and Exposition, ECCE 2009*, 330–336. <https://doi.org/10.1109/ECCE.2009.5316415>
- Tian, X., Zheng, M., & Yang, S. (2016). Maximum power point tracking for photovoltaic power based on the improved interleaved boost converter. *Proceedings of the 2016 IEEE 11th Conference on Industrial Electronics and Applications, ICIEA 2016*, 1, 2215–2218. <https://doi.org/10.1109/ICIEA.2016.7603957>
- Dwivedi, L. K., & Saket, R. K. (2017). Improve efficiency of Photovoltaic (PV) system based by PID controller. *International Research Journal of Engineering and Technology*, 4(5), 2273–2277. <https://www.irjet.net/volume4-issue05>
- Rabiaa, O., Mouna, B. H., Lassaad, S., Aymen, F., & Aicha, A. (2019). Cascade Control Loop of DC-DC Boost Converter Using PI Controller. *International Symposium on Advanced Electrical and Communication Technologies, ISAECT 2018 - Proceedings, May 2019*, 1–5. <https://doi.org/10.1109/ISAECT.2018.8618859>

Mendez-Diaz, F.; Ramirez-Murillo, H.; Garces, P.; Romero, A.; Calvente, J.; Giral, R. (2014). Control en Modo de Deslizamiento de la Tensión de Entrada del Convertidor Buck - Boost. June, 1–6

<http://deeea.urv.cat/gaei/publications.html#2014>

Mendez-Diaz, F., Ramirez-Murillo, H., Calvente, J., Pico, B., & Giral, R. (2015). Input voltage sliding mode control of the versatile buck-boost converter for photovoltaic applications. Proceedings of the IEEE International Conference on Industrial Technology, 2015-June(June), 1053–1058. <https://doi.org/10.1109/ICIT.2015.7125236>

Méndez Díaz, J. F. (2018). Desarrollo de un Sistema de Iluminación Solar Para el Ahorro de Energía Eléctrica en el Alumbrado Público de México. UNIVERSITAT ROVIRA I VIRGILI, UNIVERSIDAD POPULAR AUTONOMA DEL ESTADO DE PUEBLA <http://hdl.handle.net/10803/667293>

Mendez-Diaz, F., Pico, B., Vidal-Idiarte, E., Calvente, J., & Giral, R. (2019). HM/PWM Seamless Control of a Bidirectional Buck-Boost Converter for a Photovoltaic Application. IEEE Transactions on Power Electronics, 34(3), 2887–2899.

<https://doi.org/10.1109/TPEL.2018.2843393>

Bouchakour, A., Zaghba, L., Brahami, M., & Borni, A. (2015). Study of a Photovoltaic System Using MPPT Buck-Boost Converter. International Journal of Materials, Mechanics and Manufacturing, 3(1), 65–68. <https://doi.org/10.7763/ijmmm.2015.v3.168>

Leuchter, J., Zaplatilek, K., & Bauer, P. (2012). Photovoltaic model for circuit simulation. IECON Proceedings (Industrial Electronics Conference), 5399–5405. <https://doi.org/10.1109/IECON.2012.6389526>

Hogan, N. (2014). A general actuator model based on nonlinear equivalent networks. IEEE/ASME Transactions on Mechatronics, 19(6), 1929–1939. <https://doi.org/10.1109/TMECH.2013.2294096>

Ayop, R., & Tan, C. W. (2018). Design of boost converter based on maximum power point resistance for photovoltaic applications. Solar Energy, 160(November 2017), 322–335. <https://doi.org/10.1016/j.solener.2017.12.016>

Shanthi, N., Nivethitha, P., Sindhuja, S., Hilarini, M., & Divyabharathi, K. (2018). High Efficient Interleaved Boost Converter for Photovoltaic Applications. 7th IEEE International Conference on Computation of Power, Energy, Information and Communication, ICCPEIC 2018, 305–308. <https://doi.org/10.1109/ICCPEIC.2018.8525145>